We are IntechOpen, the world's leading publisher of Open Access books
Built by scientists, for scientists

6,900
Open access books available

185,000
International authors and editors

200M
Downloads

154
Countries delivered to

Our authors are among the

TOP 1%
most cited scientists

12.2%
Contributors from top 500 universities

BOOK CITATION INDEX
CLARIVATE ANALYTICS
INDEXED

WEB OF SCIENCE™

Selection of our books indexed in the Book Citation Index
in Web of Science™ Core Collection (BKCI)

Interested in publishing with us?
Contact book.department@intechopen.com

Numbers displayed above are based on latest data collected.
For more information visit www.intechopen.com

Geochronology From The Castelo Branco Pluton (Portugal) — Isotopic Methodologies

Antunes Imhr

Additional information is available at the end of the chapter

1. Introduction

The geochronology of granitic rocks is a key-issue in the crustal evolution and orogenic processes. Modern high precision techniques have been used to identify relevant geological episodes.

U-Th-Pb chemical dating by electron-microprobe (EPMA) is a potentially valuable method in monazite-bearing rocks. Monazite presents the fundamental conditions required to apply this procedures: 1) monazite is a U-Th enriched phase, 2) all Pb monazite is radiogenic; 3) its closure temperature has proved to be fairly high, up to 900º C [1] and 4) the system remains close [2]. Monazite presents a higher resistance than zircon to radiation damage effects [3] and low diffusion rates [4].

Different studies have demonstrated that U-Th-Pb dating by EPMA is an accurate method of geochronology (e.g., [5-8]). U-Th-Pb monazite age determination can be obtained in small crystals (5 μm), allowing the study of mineral heterogeneities, without destruction and preserving textural relationships. Microanalytical techniques are an adequate way to study magmatic and polymetamorphic events registered in monazites with zoning textures (e.g., [2, 9-11]). The advantages of this technique are the high spatial resolution and the possibility to obtain rapidly a large number of ages. The main disadvantage is the low accuracy, conditioned by Pb content and statistical treatment of data. The analytical error frequently ranges from ± 40 to ± 120Ma (2σ) for ages of 300 to 3000 Ma, respectively [8]. However, a statistical treatment of homogeneous ages promotes a decrease of uncertainty to ± 20 – 30 Ma [2].

Attemps to constraint the timing of high-temperature orogenic processes including crustal melting, metamorphism and deformation are typically based upon U-Pb age analysis of accessory minerals such as zircon and monazite. Although growth and recrystallization of

accessory minerals is being increasingly better understood in the context of the host rock petrogenesis [12-13], it remains a difficult task to related ages measured from zircon and monazite to specific orogenic events. Zircon is a very robust mineral during magmatic and metamporphic events. Very slow rates for U, Th and Pb help ensure that U-Pb age and stable isotopic and trace element compositions are preserved during subsequent deep crustal evolution. Conversely, new zircon growth associated with tectonic events post-dating the initial zircon growth typically occurs at very fine spatial scales [14]. Zircon is capable of preserving a long history of growth and modification.

Monazite also contains valuable chemical and textural information, but tends to recrystallize more readily than zircon [15-16] and thus tend to record age and stable isotopic data that are substantially different from that yielded by coexisting zircon.

ID-TIMS U–Pb age for zircon and monazite is a more accurate and precise methodology and has widely been applied. Uranium decay produces radiogenic Pb (^{207}Pb and ^{206}Pb), allowing to two independent age results-^{207}Pb/^{235}U and ^{206}Pb/^{238}U-and a dependent one-^{207}Pb/^{206}Pb [17]. Data ages were plotted on the conventional U–Pb concordia diagrams and the three obtained ages from the same mineral allows a high precision to the U-Pb system.

Radiogenic isotope ratios are commonly used as petrogenetic tracers, yielding information on time-integrated element fractionation through processes of melting, crystallization, metamorphism and contamination. The Rb–Sr dating method is based on the behavior of two mobile elements and the Rb–Sr isotope systematic of igneous rocks can be easily disturbed by fluid infiltration or during a thermal event. Isotopic Rb/Sr and Sm/Nd data are petrogenetic indicators. Initial ^{87}Sr/^{86}Sr isotopic ratio and εNd_T value of magma are a source signature and remain constant during fractionation processes [17].

Whole rock oxygen isotope (δ^{18}O) of granitic rocks will give informations about magma origin and associated magmatic crystallization and assimilation processes. Generally, magmas with no supracrustal input have an uniform oxygen isotope ratio that is distinct from magmas that assimilated or were generated directly from supracrustal sources. However, δ^{18}O can show small variations in the magmatic differentiation processes [18-24].

The Castelo Branco pluton consists of five different peraluminous granitic rocks arranged in a concentrically zoned structure [25]. This work will present the different isotopic data (U-Th-Pb, U-Pb, ^{87}Sr/^{86}Sr$_i$, εNd_T and δ^{18}O) obtained in these granitic rocks to determine their age and protolith information.

2. Castelo Branco Pluton

The Castelo Branco granitic pluton is located within the Central Iberian Zone (CIZ), the innermost zone of the Iberian Variscan Belt. This pluton is exposed over an area of 390 km^2, with a mean diameter of 19 km, and consists of five late-tectonic Variscan granitic bodies, intruding the schist-greywacke complex (CXG) (Fig. 1). In the NE border, it contacts with a medium-grained biotite granodiorite of 480 ± 2 Ma [26].

The Castelo Branco pluton generated a contact metamorphic aureole up to 2 km wide, with metasediments recrystallized as pelitic hornfels in the inner zone, and as micaschists in the outer zone. The schist–greywacke complex and the granitic rocks are cut by aplite-pegmatite dikes and quartz veins.
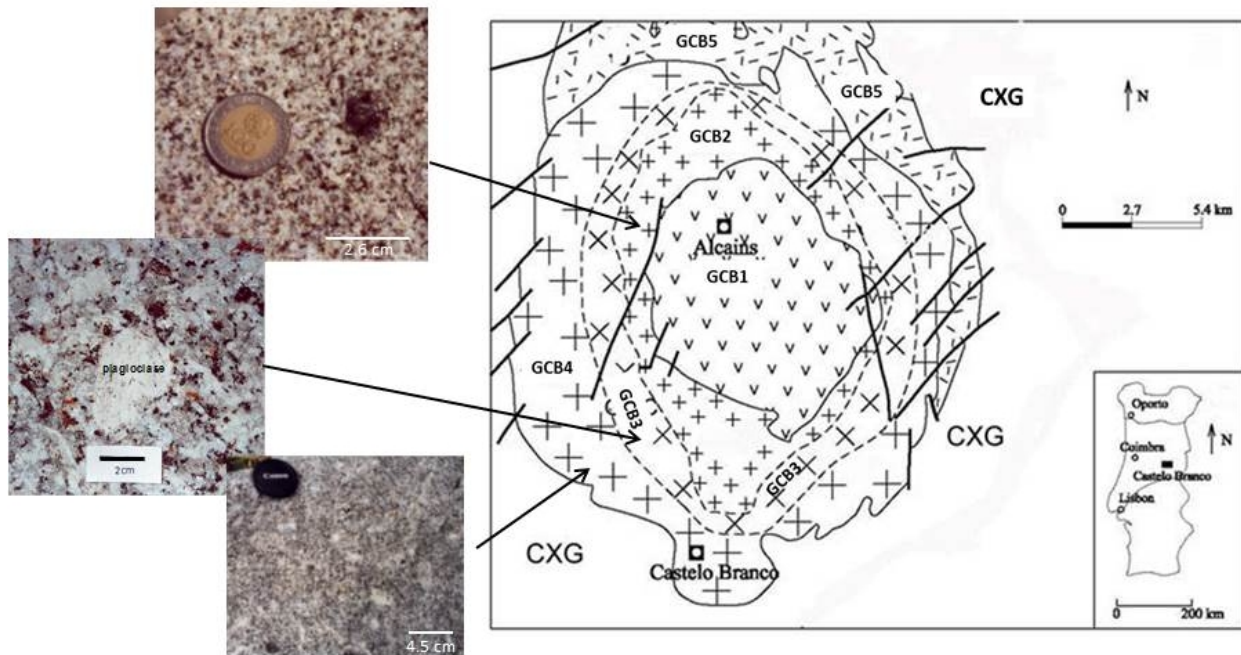

Figure 1. Geographycal setting and geological map of the Castelo Branco pluton. CXG schist–greywacke complex; GCB1 muscovite > biotite granite; GCB2 biotite > muscovite granodiorite; GCB3 biotite > muscovite granodiorite; GCB4 biotite=muscovite granite; GCB5 muscovite > biotite granite.

The medium-to fine-grained muscovite > biotite granite (GCB1) occurs at the pluton´s core and is encircled by a medium-to fine-grained, slightly porphyritic, biotite > muscovite granodiorite (GCB2), surrounded by a medium-to coarse-grained porphyritic biotite > muscovite grano-diorite (GCB3), which passes gradually to the medium-to coarse-grained, porphyritic bio-tite=muscovite granite (GCB4). Rounded enclaves of granodiorite GCB2 can be founded in the granodiorite GCB3 and granite GCB4. The boundary of the pluton is limited to N and NE by a coarse-grained muscovite > biotite granite (GCB5) (Fig. 1). The contact between granite GCB1 and granodiorite GCB2 is sharp, as is the contact between granites GCB4 and GCB5. The pluton consists of five granites concentrically distributed of 310 Ma ± 1 [25].

All the granitic rocks from the Castelo Branco pluton contain quartz, microcline, plagioclase, biotite, some chlorite, muscovite, tourmaline, monazite, apatite, zircon, ilmenite and rutile. Zircon and monazite are accessory minerals mainly included in apatite, biotite and plagioclase. Zircon occurs as euhedral crystals, whereas monazites are rounded and easily identified by their pleochroic halos.

The granitic rocks GCB1, GCB2 and GCB5 correspond to three distinct magmatic pulses derived by partial melting of heterogeneous metasedimentary materials. Granodiorite GCB3

and granite GCB4 result by fractional crystallization of plagioclase, quartz, biotite and ilmenite from the granodiorite GCB2 magma [25].

3. Analytical methodologies

3.1. U-Th-Pb EPMA

The U-Th-Pb monazite ages were calculated using U, Pb and Th monazite contents determined by electron-microprobe (EPMA). In general, monazite incorporates large amounts of Th and U during the rock formation and retains Pb of the radioactive decay processes. The obtained age will be valid if at the time of formation of the mineral, initial Pb is practically non-existent and there was no loss of Pb, Th and U [6].

The U, Pb and Th monazite contents of representative samples from the Castelo Branco pluton (Fig. 2) were determined by electron-microprobe on polished thin sections, in a Cameca SX100 at the Laboratoire of Magmas and Volcans, University Blaise Pascal (Clermont-Ferrand, France). The analytical conditions included an accelerating voltage of 15 kV and a beam current of 150 nA. The standards used were as follows: UO_2 (U Mβ), ThO_2 (Th Mα), apatite (Ca Kα, P Kα), zircon (Si Kα) and polysintetic phosphates (Y Lα, La Lα, Ce Lα, Pr Lβ, Nd Lβ, Sm Lβ, Gd Lβ). The monazite age is directly dependent on the concentrations of U, Th and Pb and its detection limit was calculated [27], with an error of 2σ associated with the uncertainty of these elements (for a confidence level of 95%) in the equation decay. The treatment of individual analysis, including Th, U and Pb contents of each monazite crystals, have been perfomed using a GwBasic computer program providing an age for each individual analysis. A statistical treatment giving the corresponding age to the studied population and the values of the sum of squared deviations (MSWD) is used for the results validation [6, 28]. If the system remained close since the early stages of crystallization, the obtained MSWD value will be less or equal to 1, whereas if the system changed flowing through interactions between minerals can promote recrystallization processes, and the MSWD value greatly increases [29].

3.2. U-Pb zircon and monazite ages

The U-Pb geochronological ages were proceeded with the preparation of zircon and monazite concentrates from representative samples of the Castelo Branco pluton. Zircon and monazite separation was carried out by a combination of magnetic separation and heavy liquids.

The preparation of the selected samples (20 to 25 kg per sample), included grinding, sieving and separation of the different granulometric fractions. After this, a subsample corresponding to the fraction below 180 mesh was selected and contains the majority of zircon and other accessory minerals. Subsequently, this subsample passed through a magnetic separator in a vertical position with a maximum speed to separate the more magnetic minerals (e.g. biotite) from the remaining fraction.

Otherwise, the less magnetic fraction is placed in a glass ampoule containing bromoform (d=2.81) to recover the heavy concentrated sample which was washed with purified water and
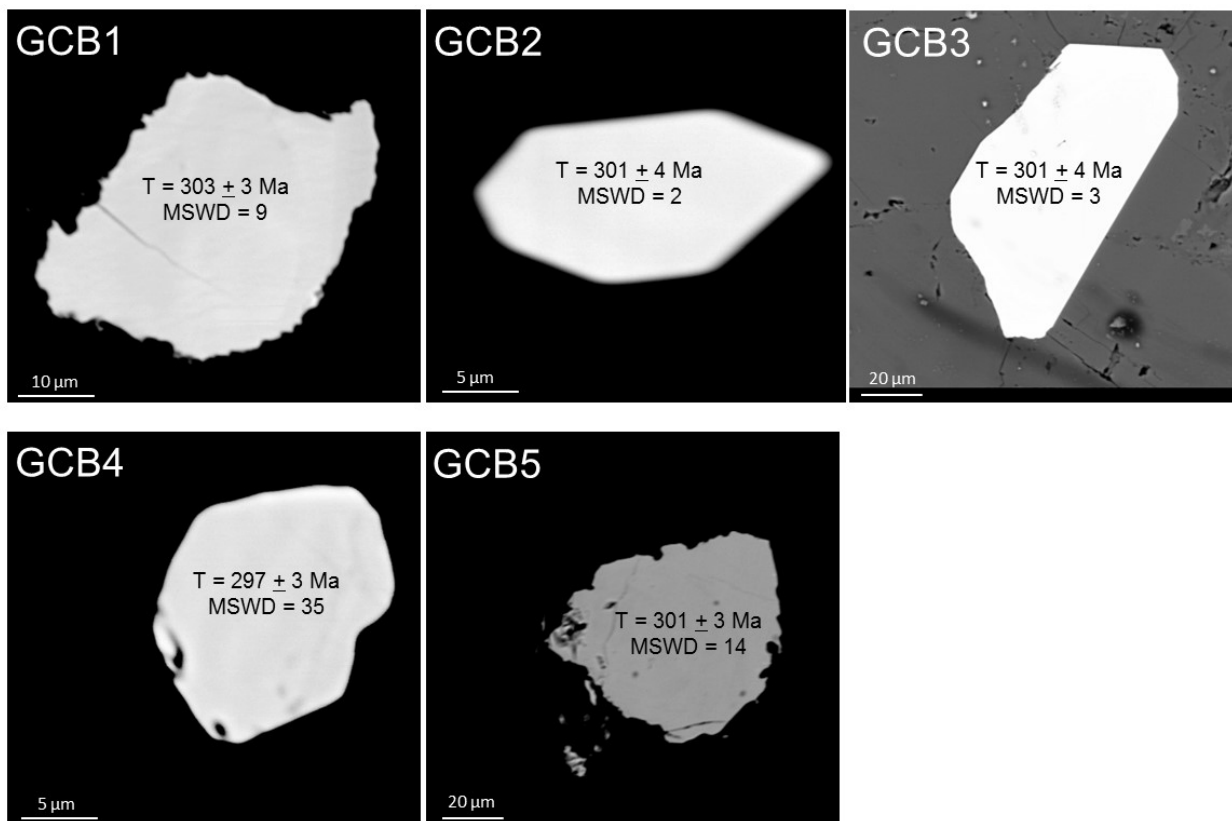
GCB1, GCB2, GCB3, GCB4 and GCB5 are those in Figure 1.

Figure 2. U-Th-Pb monazite ages from granitic rocks of Castelo Branco pluton.

acetone, and dried in an oven. After this, the concentrated sample was separated with methylene iodide (d=3.3) and the heavier fraction, which contains zircon and monazite, was washed with acetone and distilled water to eliminate methylene iodide wastes. At the end, the heavy concentrate sample was passed through a magnetic separator and different magnetic fractions containing monazite (0.8 to 1.0 A) and zircon ($\geq$ 1.7 A) were obtained. All the methodology must be carefully followed and will be fundamental for the quality of zircon concordia diagrams [30-32]. A consistent zircon concordia diagram requires non-magnetic zircon concentrates because magnetic ones are also rich in uranium, and therefore become the most likely to lost radiogenic lead and, consequently are more discordant [30].

Monazite grains for U-Pb analysis are selected from the concentrated magnetic fraction and grains free of cracks and inclusions should be used, like as to selected zircon grains. Representative crystals of zircon and monazite populations are selected by hand-picking, avoiding the fractured ones or with inclusions and, if possible, of inherited cores. However, these inherited cores are not always detectable by binocular or even optical microscope.

Selected frations of zircon and monazite were submitted to air-abrasion to prevent fracturation of the minerals, remove external portions and possible disturbances [30, 33].

The abraded crystals are washed with HNO_3 (4N), H_2O and acetone, weighted and added "spike" $^{205}Pb/^{235}U$ to dissolution processes. Zircon is dissolved with HF ($+HNO_3$) using teflon

microcapsules and heated to 185°C [34], whereas monazite is dissolved with HCl (6N) in savillex containers on a hotplate. After evaporation, HCl (3.1N) is added to each microcapsule and savillex containers, and the solution is passed through a HCl ion exchange column resin to purify U and Pb. Finally, the crystals and blank samples are placed on the filament by adding 2 drops of H_3PO_4 and silica gel.

The U–Pb isotopic results for zircon and monazite were obtained by isotope dilution thermal ionization mass spectrometry (ID-TIMS) using a Finnigan Mat 262 spectrometer at the Department of Geosciences, University of Oslo, Norway [34-37]. The initial Pb correction was done using model compositions [38] and decay constants [39]. The Isoplot program [40] was used for the plots and regression. All uncertainties relative to the analyses and ages are given at the 2σ level.

3.3. Rb-Sr, Sm-Nd and δ18O whole rock

The Sr and Nd isotope analyses were obtained at the Centro de Instrumentación Científica of the University of Granada, Spain. Samples were digested using ultraclean reagents and analyzed by thermal ionization mass spectrometry (TIMS), using a Finnigan Mat 262 spectrometer, after chromatographic separation with ion-exchange resins [41].

The standardized ratios $^{86}Sr/^{88}Sr=0.1194$ and $^{146}Nd/^{144}Nd=0.7219$ and blank values for Sr and Nd were of 0.6 and 0.09 ng, respectively. The external precision of the method (2σ) was estimated by ten successive samples corresponding to different attacks in the same standard sample WSE [42]. This value can be considered as a laboratory error, since it includes both the different attacks and chemical separation of the various samples, as well as the instrumental error of the determinations. The obtained errors were $^{87}Sr/^{86}Sr=0.706596 \pm 0.000018$ (2σ=0.0026 %) and $^{143}Nd/^{144}Nd=0.512467 \pm 0.0000084$ (2σ=0.0016 %). On the analysis, the NBS 987 was used as a standard solution, with a reproducibility for repeated measurements of $^{87}Sr/^{86}Sr=0.71025 \pm 0.0000046$ (2 σ=0.0065 %). The reproducibility obtained for the La Jolla standard was $^{143}Nd/^{144}Nd=0.511845 \pm 0.0000072$ (2σ=0.0014 %). The isotopic ratios $^{87}Rb/^{86}Sr$ and $^{147}Sm/^{144}Nd$ were determined with an accuracy better than ± 1.2 % and ± 0.9 % (2σ), respectively. Regression lines of $^{87}Rb/^{86}Sr$ versus $^{87}Sr/^{86}Sr$ were calculated using the least-squares method [43], implemented in the Isoplot program [40]. Errors are quoted at the 95% confidence level and are 2σ.

The isotopic results of δ18O whole rock of the five granitic rocks were obtained in the Department of Earth Sciences, University of Western Ontario (Canada), using conventional extraction line and trifluoride chlorine as a reactant. This method has an accuracy of ± 0.2 ‰ and patterns such as quartz and CO_2 laboratory were used.

4. Isotopic geochronology

4.1. U-Th-Pb (EPMA) monazite ages

U-Th-Pb contents of selected monazite grains from the five granitic rocks of the Castelo Branco pluton were determined by EPMA and calculated monazite ages (Table I). A total of 195 U-

Th-Pb analyses (EPMA) of monazite were obtained from the granitic rocks of the Castelo Branco pluton. Monazite crystals are homogeneous and unzoned (Fig. 2) and a distinct age between core and rim was not found. Therefore, an individual age were considered to the analysed grains.

Monazites from GCB1 present the highest Pb and U contents of granitic rocks from the Castelo Branco pluton (Table I). Monazite age data obtained from two samples of GCB1 granite apparently show a great dispersion, but if the errors obtained are taken into account the ages are similar. Lead, U and Th average contents from monazite crystals of granodiorites GCB2 and GCB3 and granite GCB4 show variation but within a similar range (Table I). Otherwise, monazite from granite GCB5 contains higher Pb and U contents than monazites from granodiorites GCB2 and GCB3 and granite GCB4 (Table 1).

Sample	Pb (ppm) ± σ	U (ppm) ± σ	Th (ppm) ± σ	T (Ma) ± σ	N	Average Age		
						T (Ma)	MSWD	N
GCB1								
GCL7	1402 ± 32	18012 ± 96	49401 ± 207	297 ± 7	19	303 ± 9	9	31
GEB2	1791 ± 38	18590 ± 80	64369 ± 206	310 ± 17	12			
GCB2								
GIN	666 ± 28	6205 ± 73	28751 ± 195	304 ± 15	7	301 ± 4	2	38
GIN2	948 ± 19	7028 ± 33	48451 ± 94	297 ± 6	31			
GCB3								
REPB	1043 ± 20	6566 ± 39	5595 ± 112	301 ± 4	32	301 ± 4	3	32
GCB4								
GM	768 + 31	2740 + 74	48670 + 262	297 + 14	16	297 + 3	35	45
NAC	1231 ± 23	7439 ± 31	67602 ± 90	300 ± 6	29			
GCB5								
LARDO	1285 + 22	13178 + 52	50581 + 85	301 + 3	49	301 + 3	14	49

GCB1, GCB2, GCB3, GCB4 and GCB5 are those in Figure 1. N – Number of analysis.

Table 1. EPMA U-Th-Pb monazite data from granitic rocks of the Castelo Branco pluton

The obtained results of monazite from the granite GCB4 reveal heterogeneity, supported by the higher MSWD values observed which may be associated with the uncertainties of this methodology [44]. However, they may also be related to the occurrence of geological processes responsible for the presence of some initial Pb in monazite grains or alteration processes.

The U-Th-Pb monazite age obtained by electron microprobe is an important alternative geochronological method, which allows to obtain accurate and similar results to those obtained by isotopic dating ages [8]. The potentiality of this geochronological methodology increases

with the application togheter with other isotopic dating methods, such as U-Pb zircon and monazite [7].

The monazite ages obtained through U-Th-Pb (EPMA) do not allow themselves to evaluate the accuracy of obtained ages because there is concordance between Th-Pb and U-Pb systems. However, the consistency of the obtained measurements allows to conclude that a crystal was not significantly altered or modified [7]. The most recent monazite age values obtained by EPMA may indicate an isotopic discordance leading to a more relatively recent age with a smaller ratio Pb/(Th+U) [45]. U-Th-Pb (EPMA) monazite age correponds to the minimum $^{207}Pb/^{235}U$ age and maximum $^{208}Pb/^{232}Th$ age. However, these isotopic disagreements are not possible to assess by electron microprobe [45].

Monazites from granites GCB1 and GCB5 and granodiorites GCB2 and GCB3 presented the ages of 301-303 Ma, whereas monazite from the granite GCB4 tends to be more recent (297 Ma; Table 1). However, the various ages are similar and within the range of the analytical error. The highest MSWD values on monazites from granodiorite GCB4 and granite GCB5 must be associated with a disperion of the results, which could be related to the methodology uncertainty or to a possible geological or alteration processes.

4.2. U-Pb zircon and monazite ages

U–Pb isotopic analyses were carried out on zircon and monazite from representative samples of the granitic rocks GCB1, GCB2 and GCB5 from the Castelo Branco pluton using the ID-TIMS method [25].

Granodiorite GCB1 contains hyaline or colorless zircons, euhedral elongated prismatic and subhedral crystals with varied size and forms. Some of them contain associated fractures and rare inclusions (Fig. 3a).

Monazite crystals (Fig. 3b) are reversely discordant, which can be associated with Paleozoic geological processes and $^{207}Pb/^{235}U$ concordant monazite age should be used (Table 2). The reversly concordia can be interpreted as the result of the existence of some inherited Pb, associated with an excess of initial ^{230}Th [46-47] due to possible inherited zircon cores. For other authors, it could be justified with some degree of change [36] or incomplete dissolution [37]. Some zircons have inherited cores and were not considered for the U-Pb age. The age $^{207}Pb/^{206}Pb$ of 309.9 ± 1.0 Ma was obtained for a more concordant zircon crystal and is similar to the zircon concordia age 309.9 ± 1.1 Ma (Fig. 4; Table 2). Monazite from granite GCB1 plots slightly reversely discordant (Fig. 4), a fact commonly linked to ^{230}Th initial excess, which eventually results in an excess of ^{206}Pb and reverse discordance [46-47]. The $^{207}Pb/^{235}U$ ratio is not affected by this disequilibrium effect and can be used as the closest estimate for monazite age. The concordant monazite of granite GCB1 yields a $^{207}Pb/^{235}U$ age 309.5 ± 0.9 Ma, which overlaps the zircon crystal of the granite GCB1 (Fig. 4; Table 2).

Zircons from granodiorite GCB2 occur as hyaline to slightly pinkish, elongated prismatic crystals or subhedral crystals with longitudinal cracks and occasional inclusions (Fig. 3c). Monazite is euhedral with rare inclusions (Fig. 3d). Zircon crystals from the granodiorite GCB2 plot near the concordia, but one of them presents a restitic core and deviates from the curve
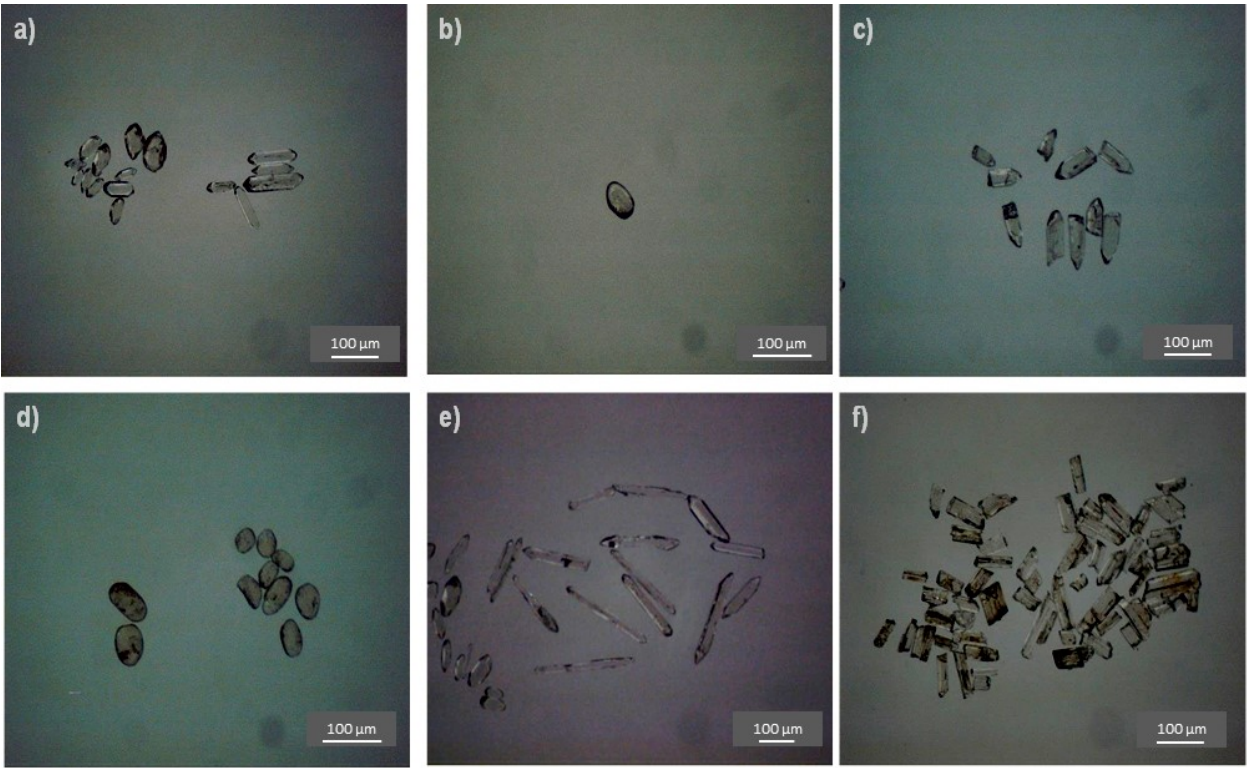
Figure 3. Selected zircon and monazite crystals from granitic rocks of Castelo Branco pluton. Muscovite > biotite granite GCB1: zircon (a), monazite (b); biotite > muscovite granodiorite GCB2: zircon (c) monazite (d); muscovite > biotite granite GCB5: zircon (e, f).

(Fig. 4). So, the concordia age was not considered. The concordant zircon yields a ^{207}Pb/^{206}Pb age of 310.1 ± 0.8 Ma (Fig. 4; Table 2). The projection of monazite fraction is slightly above the concordia curve and gives an age of 310.6 ± 1.5 Ma, obtained by ^{207}Pb/^{235}U ratio (Fig. 4; Table 2). The age of 310.1 ± 0.8 Ma obtained from the concordant zircon crystal should be considered for the granodiorite GCB2 Table 2.

	GCB1	GCB2	GCB5
Zircon concordia age	309.9 ± 1.1 Ma MSWD = 1.11	-	309.1 ± 0.6 MSWD = 0.11
^{207}Pb/^{206}Pb concordant zircon age	309.9 ± 1.0 Ma	310.1 ± 0.8 Ma	309.7 ± 0.4 Ma
^{207}Pb/^{235}U concordant monazite age	309.5 ± 0.9 Ma	310.6 ± 1.5 Ma	309.7 ± 0.4 Ma

GCB1, GCB2 and GCB5 as in Figure 1.

Table 2. U-Pb zircon and monazite ages of granitic rocks from the Castelo Branco pluton

Granite GCB5 contains hyaline and colorless elongated prismatic zircons and several subhedral crystals and some slightly rounded, corresponding to fractions or fragmented crystals,
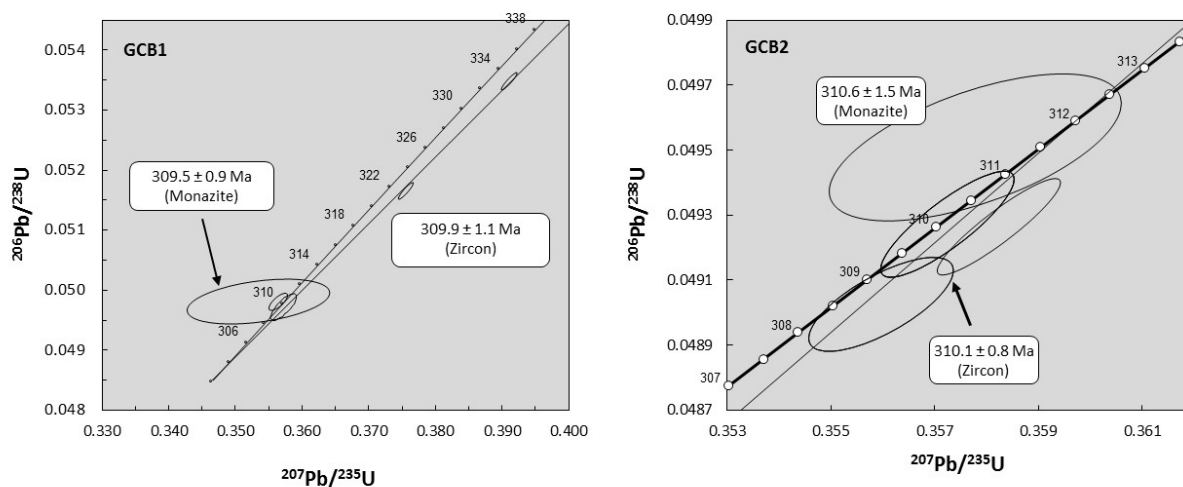
Figure 4. Selected concordia ^{207}Pb/^{235}U versus ^{206}Pb/^{238}U diagrams for zircon and monazite of muscovite > biotite granite GCB1 and biotite > muscovite granodiorite GCB2 from the Castelo Branco pluton (Error for ellipses are drawn at 2σ).

some brownish colourless with inclusions (Fig. 3e; 3f). Monazite is unsual and with rare inclusions. The zircon crystals define a discordia line yielding a lower intersect age of 309.1 ± 0.6 Ma (MSWD=0.11), similar to the ^{207}Pb/^{206}Pb concordant zircon age (309.7 ± 0.4 Ma), and an upper intersect age of about 1000 Ma. Concordant monazite has a ^{207}Pb/^{235}U similar age of 309.7 ± 0.4 Ma (Table 2).

The average U-Pb age obtained for each granite from the Castelo Branco pluton is similar (310 Ma), indicating that they are contemporaneous (Table 2).

Zircon from granite GCB5 is the richest in U content (GCB5 511 ppm) of granitic rocks from Castelo Branco pluton (GCB1 384 ppm; GCB2 411 ppm) and with the highest ^{206}Pb/^{204}Pb ratio (GCB1 7932; GCB2 4571; GCB5 23130). Monazite from GCB5 also presents the highest ^{206}Pb/^{204}Pb ratio (GCB1 1281; GCB2 1340; GCB5 7409) [25]. Zircon Th/U ratio from granitic rocks of Castelo Branco pluton ranges between 0.10 – 0.88, corresponding to zircons with an igneous signature [48]. Zircon from granodiorite GCB2 presents the highest Th/U variation range (Th/U 0.18-0.88) including the values obtained from granodiorite GCB1 zircon (Th/U 0.10-0.28) and granite GCB5 (Th/U 0.11-0.14). The selected monazite crystals from granite GCB1 show the highest variability U and Th/U results including the highest and the lowest value of U (U 159 – 4514 ppm) and Th/U ratio (4.58 – 109.34) from the granitic rocks of the Castelo Branco pluton.

The discordant monazites tend to have higher levels of Th, identified by the highest values of Th/U ratio [36]. However, although high Th values may contribute to the discrepancy associated with monazite crystals is not possible to establish a linear correlation between Th/U ratio and the degree of monazites discordance. In some monazite crystals, U-Pb ratio and presented features could have a greater influence on the associated discordance [36]. The discordance of monazite crystals from granite CBG5 could be associated with ^{230}Th disequilibrium and U loss, which can be justified by possible crystal change, as found in monazites from Suomujärvi

Complex [36]. In monazite crystals, there are considerable amounts of Pb and Th that could be incorporated and the enrichment or depletion of U will depend on fluid composition and associated processes [49].

The U-Pb monazite and U-Th-Pb isotopic data confirm that the Castelo Branco pluton consists of five concentric late-tectonic Variscan granitic bodies, which intruded the Cambrian schist – greywacke.

4.3. Rb-Sr, Sm-Nd and $\delta^{18}O$ whole rock

For Rb-Sr and Sm-Nd isotopic studies, representative samples of the five granitic rocks from the Castelo Branco pluton were selected, after a detailed geological field study, petrographic and geochemical whole rock data interpretation. The Rb/Sr isotopic age obtained for granitic rocks from Castelo Branco pluton (300 ± 24 Ma; [50]) is lower than the U-Pb zircon and monazite ages (310 Ma; Table 2), which could be atributed to an opening of the Rb-Sr system during the metamorphic event associated with late-D3 granite intrusions, or furthermore to the lower temperature of Rb-Sr system than U-Pb system [23]. Initial ($^{87}Sr/^{86}Sr$) ratios and εNd_T values were calculated using the U-Pb age of 310 Ma (Table 3). Petrographic and geochemical characteristics of granodiorite GCB3 and granite GCB4 suggest that they are related to granodiorite GCB2, and a similar age of 310 Ma have been considered.

	GCB1	GCB2	GCB3	GCB4	GCB5
($^{87}Sr/86Sr)_{310}$	0.7082 – 0.7098	0.7085 – 0.7128	0.7104	0.7078 – 0.7104	0.7120
εNd_{310}	-3.8 ± 0.2	-1.7 ± 0.4	-0.8	-2.8 ± 0.68	-3.0
T_{DM}	1.64 ± 0.12	1.10 ± 0.0	1.11	1.35 ± 0.1	1.56
$\delta^{18}O$ (‰)	13.53 ± 0.11	12.27 ± 0.04	12.50	12.75	12.91 ± 0.23

GCB1, GCB2, GCB3, GCB4 and GCB5 as in Figure 1.

Table 3. εNd_{310} and $\delta^{18}O$ data of granitic rocks from the Castelo Branco pluton

The ($^{87}Sr/^{86}Sr)_{310}$ ratios obtained for granite GCB1, granodiorite GCB2 and granite GCB5 are characteristic of granites resulting from crustal anatexis of metasedimentary rocks (Table 3).

The εNd_{310} and T_{DM} values obtained for representative samples from granitic rocks of Castelo Branco pluton were calculated [51] with a ^{147}Sm desintegration constant of $\lambda = 6.54 *10^{-12}$ year^{-1} [52]. To εNd_T and T_{DM} calculation $^{143}Nd/^{144}Nd_{CHUR} = 0.512638$ and $^{147}Sm/^{144}Nd_{CHUR} = 0.1967$ [53] and $^{143}Nd/^{144}Nd_{DM} = 0.513151$ and $^{147}Sm/^{144}Nd_{DM} = 0.22$ [54] were applied, respectively.

Granites GCB1 and GCB5 show lower values of εNd_{310} and higher values of T_{DM} than grano-diorites GCB2, GCB3 and granite GCB4 (Table 3), suggesting that GCB1 and GCB5 granites are not relate to the granodiorites GCB2 and GCB3 and granite GCB4 from the Castelo Branco pluton.

The diagram εNd_{310} versus $(^{87}Sr/^{86}Sr)_{310}$ shows a dominantly crustal origin for all granitic rocks from the Castelo Branco pluton. All samples plot on the field IV, indicating that are derived from Rb enriched and depleted Sm protoliths (Fig. 5a). The scatter of $(^{87}Sr/^{86}Sr)_{310}$ ratio suggests that the granitic rocks were not in complete isotopic equilibrium at the time of formation, which is also supported by an heterogeneous εNd_{310} (Fig. 5a).
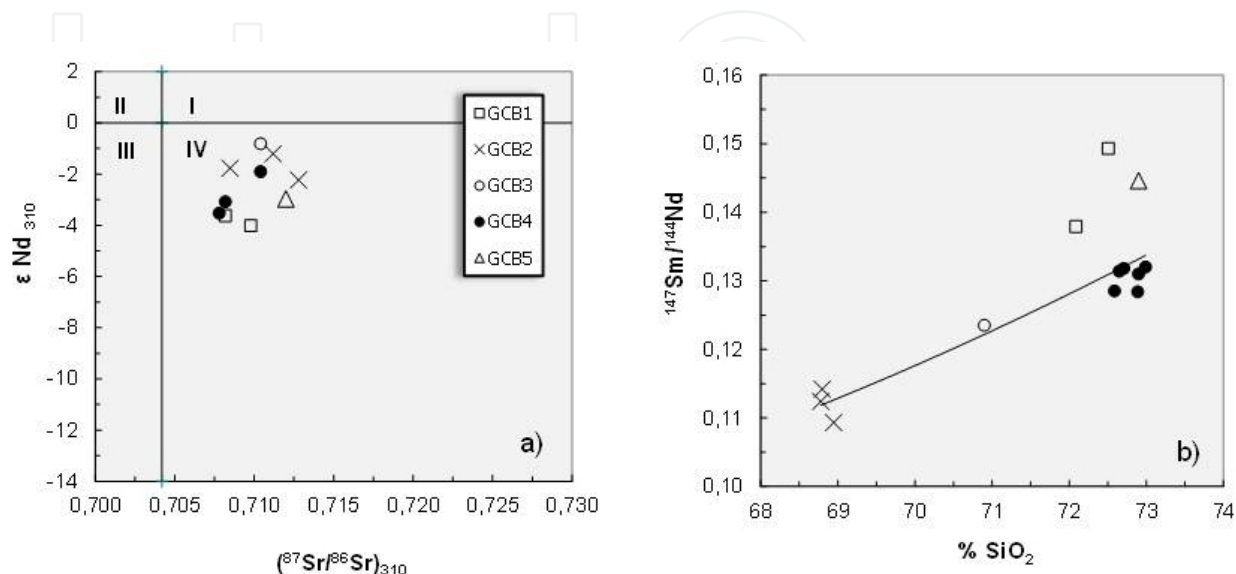

Figure 5. Selected diagrams of granitic rocks from Castelo Branco pluton: a) εNd_{310} versus $(^{87}Sr/^{86}Sr)_{310}$; b) $^{147}Sm/^{144}Nd$ versus SiO_2. GCB1, GCB2, GCB3, GCB4 and GCB5 as in Figure 1.

The obtained results show coherence within each of the five granitic rocks from the Castelo Branco pluton with a slightly evolutionary trend from higher to lower values of $(^{87}Sr/^{86}Sr)_{310}$ and εNd_{310} from granodiorite GCB2 and GCB3 to granite GCB4 [25]. Granites GCB1 and GCB5 tend to have the most negative values for εNd_{310}, with variable $(^{87}Sr/^{86}Sr)_{310}$. These distributions suggest the contribution of at least three magmatic components GCB1, GCB2 and GCB5 with different isotopic signatures (Table 3; Fig. 5a). All the data plot within a field delimited by $\varepsilon Nd = -1$ to -4 and $^{87}Sr/^{86}Sr = 0.708-0.712$, which indicate derivation from crustal material with average Mesoproterozoic mantle extraction ages (Fig. 5a). T_{DM} values of granitic rocks are similar to the T_{DM} data for schist-greywacke complex from the studied area [55].

The $^{147}Sm/^{144}Nd$ versus SiO_2 diagram of granitic rocks from the Castelo Branco pluton shows a positive correlation with an increase of $^{147}Sm/^{144}Nd$ from granodiorite GCB2, to granodiorite GCB3 and granite GCB4. Otherwise, granites GCB1 and GCB5 do not present similar variation and plot outside the straight line (Fig. 5b).

Whole rock oxygen-isotope ($\delta^{18}O$) values, obtained for eight representative samples of granitic rocks from the Castelo Branco pluton, range from +12.27 to +13.53 ‰ (Table 3). The obtained $\delta^{18}O$ values are higher than 10 ‰, indicating that the granitic rocks from the Castelo Branco pluton correspond to S-type granites [56].

There is a progressive increase of $\delta^{18}O$ from granodiorite GCB2 to granodiorite GCB3, granite GCB4 and granite GCB5. The $\delta^{18}O$ values are also positively correlated with SiO_2,

Li, Rb and negatively correlated with FeO, Sr and Ba [25]. In these diagrams, granodiorite GCB2 and GCB3 and granite GCB4 define a curvilinear variation trend which is characteristic of a magmatic differentiation process. Granite GCB1 yields the highest value, which deviates clearly from the trend, whereas granite GCB5 plots closer, but in average has higher $\delta^{18}O$ than the trend [25].

A system without contamination will present radiogenic isotopic characteristics similar to the original source, even with the occurence of magmatic differentiation processes [17]. However, the values of $\delta^{18}O$ show small variations in the magmatic differentiation processes, with an increase of about 1 to 1.2 ‰, increasing with the degree of differentiation [18-24]. The $\delta^{18}O$ values increase from the granodiorite GCB2 (12.27 ‰) to the granodiorite GCB4 (12.75 ‰), which is associated with the fractional crystallization process [24].

These isotopic ratios ($^{87}Sr/^{86}Sr)_{310}$, εNd_{310} and $\delta^{18}O$ values of granite GCB1, granodiorite GCB2 and granite GCB5 are of granites originated from crustal anatexis of metasedimentary rocks [25].

5. Conclusions

U-Th-Pb monazite ages from granodiorite GCB1 and granite GCB5 and granodiorites GCB2 and GCB3 have a similar values, ranging from 303-301 Ma. Granodiorite GCB4 presents a lower value of 297 ± 3 Ma, but the difference is inside the analytical error. However, U-Th-Pb monazite ages for granodiorites GCB1 and GCB2 and granite GCB5 are consistently below about 7 MA, with respect to the age of 310 ± 1 Ma obtained by ID-TIMS U-Pb zircon and monazite.

The most recent ages obtained by U-Th-Pb monazite EPMA age could be associated to the higher levels of U and Th and lower Th/U ratio obtained by electron microprobe relatively to those obtained by ID-TIMS, as well as Pb partial loss like as found in rocks of southern India [1]. The U-Pb zircon and monazite isotopic ages (ID-TIMS) are the most accurate. However, U-Th-Pb monazite ages (EPMA) are closer.

The granitic rocks GCB1, GCB2 and GCB5 correspond to three distinct magmatic pulses and have a similar age of 310 ± 1 Ma (ID-TIMS U-Pb zircon and monazite). These three granitic rocks have different ($^{87}Sr/^{86}Sr)_{310}$, εNd_{310} and $\delta^{18}O$ values and correspond to three distint magmatic pulses derived by partial melting of heterogeneous metasedimentary materials.

Acknowledgements

Author details

Antunes Imhr[1,2,3]

Address all correspondence to: imantunes@ipcb.pt

1 Polytechnic Institute of Castelo Branco and Geo-Environmental and Resources Research Center, Portugal

2 Neiva AMR, Department of Earth Sciences and Geosciences Centre, University of Coimbra, Portugal

3 Silva MMVG, Department of Earth Sciences and Geosciences Centre, University of Coimbra, Portugal

References

[1] Braun I, Montel JM, Nicollet C. 1998. Electron microprobe dating of monazites from high-grade gneisses and pegmatites of the Kerala Khondalite Belt, southern India. Chem. Geol. 146, 65-85.

[2] Orejana D, Merino E, Villaseca C, Pérez-Soba C, Cuesta A. 2012. Electron microprobe monazite geochronology of granitic intrusions from the Montes de Toledo batholith (central Spain). Geol. J. 47, 41-58.

[3] Meldrum A, Boatner LA, Weber WJ, Ewing RC. 1998. Radiation damage in zircon and monazite. Geochim. Cosmich. Acta 62, 2509-2520.

[4] Cherniak DJ, Watson EB, Grove M, Harrison TM. 2004. Pb diffusion in monazite: a combined RBS/SIMS study. Geochim. Cosmochim. Acta 68, 829-840.

[5] Suzuki K, Adachi M. 1994. Middle precambrian detrital monazite and zircon from the Hida gneiss on Oki-Dogo Island, Japan: their origin and implications for the correlation of basement gneiss of southwest Japan and Korea. Tectonophysics 235, 277-292.

[6] Montel JM, Foret S, Veschambre M, Nicollet C, Provost A. 1996. Electron microprobe dating of monazite. Chem. Geol. 131, 37-53.

[7] Williams ML, Jercinovic MJ. 2002. Microprobe monazite geochronology: putting absolute time into microstructural analysis. J. Struct. Geol. 24, 1013-1028.

[8] Cocherie A, Mezeme EB, Legendre O, Fanning CM, Faure M, Rossi P. 2005. Electron-microprobe dating as a tool for determining the closure of Th–U–Pb systems in migmatitic monazites. Am. Mineral. 90, 607–618.

[9] Harrison TM, McKeegan KD, Le Fort P. 1995. Detection of inherited monazite in the Manaslu leucogranite by [208]Pb/[232]Th ion microprobe dating: crystallization age and tectonic implications. Earth Plant. Sci. Lett. 133, 271-282.

[10] Cocherie A, Legendre O, Pecaut JJ, Kouamelan AN. 1998. Geochronology of polygenetic monazites constrained by in situ electron microprobe Th-U-total lead determination: implications for lead behaviour in monazite. Geochim. Cosmochim. Acta 62, 2475-2497.

[11] Be Mezene E, Cocherie A, Faure M, Legendre O, Rossi P. 2006. Electron microprobe monazite geochronology of magmatic events examples from Variscan migmatites and granitoids, Massif Central, France. Lithos 87, 276-288.

[12] Kohn MJ, Malloy MA. 2004. Formation of monazite via prograde metamorphic reactions among common silicates: implications for age determinations. Geochim. Cosmochim. Acta 68, 101-113.

[13] Kelsey DE, Clark C, Hand M. 2008. Thermobarometric modeling of zircon and monazite growth in melt-bearing systems: examples using model metapelitic and metapsammitic granulites. J. Metam. Geol. 26, 199-212.

[14] Corfu F, Hanchar JM, Hoskin PWO, Kinny P. 2003. Atlas of zircon textures. In: Hanchar JM, Hoskin PWO (Eds). Zircon, Rev. Miner. Geochem. 53, 469-500.

[15] Ayres JD, Loflin M, Miller CF, Barton MD, Coath CD. 2006. In site oxygen isotope analysis of monazite as monitor of fluid infiltration during contact metamorphism: Birch Creek Pluton aureole, White Mountains, Eastern California. Geol. 34, 553-656.

[16] Harlov DE, Wirth R, Hetherington CJ. 2007. The relative stability of monazite and huttonite at 300-900ºC and 200-1000MPa: metasomatism and the propagation of metastable mineral phases. Am. Mineral. 92, 1652-1664.

[17] Rollinson H. 1993. Using Geochemical Data: Evalution, Presentation and Interpretation. Longman, UK. 352 pp.

[18] Taylor Jr HP, Epstein S. 1962. Relationships between ^{18}O/^{16}O ratios in coexisting minerals of magmatic and metamorphic rocks: Part I. Principles and experimental results. Geol. Soc. Amer. Bull. 73, 461-480.

[19] Epstein S, Taylor HP Jr. 1972. [18]O/^{16}O, [30]Si/[28]Si, ^{13}C/^{12}C and D/H studies of Apollo 14 and 15 samples, Proc. 3rd Lunar Sci. Conf. Geochim. Cosmochim. Acta, Suppl. 3/2, 1429.

[20] Muehlenbachs K, Byerly G. 1982. ^{18}O-Enrichment of silicic magmas caused by crystal fractionation at the Galapagos Spreading Center. Contrib. Mineral. Petrol. 79, 76-79.

[21] Kalamarides RI. 1984. Kiglapait geochemistry VI: oxygen isotopes. Geochim. Cosmochim. Acta 46, 1863-1868.

[22] Sheppard MF, Harris C. 1985. Hydrogen and oxygen isotope geochemistry of ascension Island lavas and granites: variation with crystal fractionation and interaction with sea water. Contrib. Mineral. Petrol. 91, 74-81.

[23] Faure G. 1986. Principles of isotope geology. John Willey & Sons, New York. 589 pp.

[24] White 2003. High temperature applications II: oxygen isotopes as an indicator of assimilation. Geol. 656 Isotope Geochemistry. Lectures 30, 227-231.

[25] Antunes IMHR, Neiva AMR, Silva MMVG, Corfu F. 2008. Geochemical and isotopic data on the granitic-granodioritic, concentrically zoned Castelo Branco pluton (central Portugal). Lithos 103 (3/4), 445-465.

[26] Antunes IMHR, Neiva AMR, Silva MMVG, Corfu F. 2009. The genesis of I-and S-type granitoid rocks of the Early Ordovician Oledo pluton, Central Iberian Zone (central Portugal). Lithos 111 (3/4), 168-185.

[27] Ancey M, Bastenaire F, Tixier R. 1978. Application des méthodes statistiques in microanalyse. In: Maurice F, Menyard L, Tixier R. (Eds.), Microanalyse-Microscope Électronique à Balayage Orsay: Les éditions des Physicien, 323-347.

[28] Montel JM, Veschambre M, Nicollet C. 1994. Datation de la monazite à la microsonde electronique (Dating monazite using electron microprobe). Comp. Rend. L'Académie Sci. 318, 1489-1495.

[29] Cocherie A, Albarède F. 2001. An improved U-Th-Pb age calculation for electron microprobe dating of monazite. Geochim. Cosmochim. Acta 65, 4509-4522.

[30] Krogh TE. 1982. Improved accuracy of U–Pb zircon ages by creation of more concordant systems using an air abrasion technique. Geochim. Cosmochim. Acta 46, 637-649.

[31] Tucker RD, Raheim A, Krogh TE, Corfu F. 1987. Uranium-lead zircon and titanite ages from the northern portion of the Western Gneiss Region, south-central Norway. Earth Planet. Sci. Lett. 81, 203-211.

[32] Davidson A, Van Breemen O. 1988. Baddedeleyite-zircon relationships in coronitic metagrabro, Grenville Province, Ontario: Implications for geochronology. Contrib. Mineral. Petrol. 100, 291-299.

[33] Davis DW, Blackburn CE, Krogh TE. 1982. Zircon U-Pb ages from the Wabigoon, Manitou Lakes Region, Wabigoon Subprovince, northwest Ontario. Can. J. Earth Sci. 19, 254-266.

[34] Krogh TE. 1973. A low contamination method for hydrothermal decomposition of zircon and extraction of U and Pb for isotopic age determination. Geochim. Cosmochim. Acta 37, 485-494.

[35] Corfu F, Andersen TB. 2002. U–Pb ages of the Dalsfjord Campus, SW-Norway, and their bearing on the correlation of the allochthonous crystalline segments of the Scandinavian Caledonides. Int. J. Earth Sci. 91, 955–963.

[36] Corfu F, Evins PM. 2002. Late Paleoproterozoic monazite and titanite U–Pb ages in the Archean Suomujäri complex, N Finland. Prec. Res. 116, 171-181.

[37] Corfu F. 2004. U–Pb geochronology of the Lekres Group: an exotic Early Caledonian metasedimentary assemblage stranded on Lofoten basement, northern Norway. J. Geol. Soc. (Lond.) 161, 619-627.

[38] Stacey JS, Kramers JD. 1975. Approximation of terrestrial lead isotope evolution by a two-stage model. Earth Planet. Sci. Lett. 34, 207-226.

[39] Jaffey AH, FlynnKF, Glendenin LE, Benthey WC, Essling AM. 1971. Precision measurement of half lives and specific activities of ^{235}U and ^{238}U. Phys. Rev., C Nucl. Phys. 4, 1889-1906.

[40] Ludwig KR. 1999. Isoplot/Ex version 2.03. A geochronological toolkit for Microsoft Excel. Berkeley Geochronology under Special Publication, vol. 1 43 pp.

[41] Montero P, Bea F. 1998. Accurate determination of ^{87}Rb/^{86}Sr and ^{147}Sm/^{144}Nd by inductively coupled plasma mass spectrometry in isotope geoscience: an alternative to isotope dilution analysis. Anal. Chim. Acta 358, 22-233.

[42] Govindaraju K, Potts PJ, Webb PC, Watson JS. 1994. Report on Whin Sill Dolerite W-E from England and Pitscurrie Microgabbro PM-S from Scotland: assessment by one hundred and four international laboratories. Geostand. Newslett. 18, 211-300.

[43] York D. 1969. Least-squares fitting of a straight line with correlated error. Earth Planet. Sci. Lett. 5, 320-324.

[44] Pyle JM, Spear FS, Wark DA, Daniel CG, Storm LC. 2005. Contributions to precision and accuracy of monazite microprobe ages. Am. Mineral. 90, 547-577.

[45] Kuiper YD. 2005. Isotopic age constraints from electron microprobe U-Th-Pb dates using a three-dimensional concordia diagram. Am. Mineral. 90, 586-591.

[46] Schärer U. 1984. The effect of initial ^{230}Th disequilibrium on young U–Pb ages: the Makalu case, Himalaya. Earth Planet. Sci. Lett. 67, 191-204.

[47] Kalt A, Corfu F, Wijbrans JR. 2000. Time calibration of a P–T path from a Variscan high-temperature low-pressure metamorphic complex (Bayerische Wald, Germany) and the detection of inherited monazite. Contrib. Mineral. Petrol. 138, 143-163.

[48] Williams IS, Claesson S. 1987. Isotopic evidence for the Precambrian provenance and Caledonian metamorphism of high grade paragneisses from the Seve Nappes, Scandinavian Caledonides. II. Ion microprobe zircon U-Th-Pb. Contrib. Mineral. Petrol. 97, 205 – 217.

[49] Poitrasson F, Chenery S, Bland DJ. 1996. Contrasted monazite hydrothermal altera-
tion mechanisms and their geochemical implications. Earth Planet. Sci. Lett. 145,
79-96.

[50] Antunes IMHR, 2006. Mineralogia, Geoquímica e Petrologia de rochas granitóides da
área de Castelo Branco-Idanha-a-Nova. Unpublished PhD. thesis. University of
Coimbra, Portugal, 453 pp.

[51] De Paolo DJ. 1981. Trace elements and isotopic effects of combined wall rock assimi-
lation and fractional crystallization. Earth Planet. Sci. Lett. 53, 189–202.

[52] Steiger RH, Jäger E. 1977. Convention of the use of decay constants in geo and cos-
mochronology. Earth Planet. Sci. Lett. 36, 359-362.

[53] Jacobsen SB, Wasserburg GJ. 1980. Sm-Nd isotopic evolution of chondrites and
achondrites. Earth Planet. Sci. Lett. 67, 137-150.

[54] Liew TC, Hofmann AW. 1988. Precambrian crustal components, plutonic associa-
tions, plate environment of the Hercynian Fold Belt of Central Europe: indications
from a Nd and Sr isotopic study. Contrib. Mineral. Petrol. 98, 129-138.

[55] Beetsma JJ. 1995. The late Proterozoic/Paleozoic and Hercynian crustal evolution of
the Iberian Massif, N Portugal. Unpublished PhD. thesis. Vrije Universiteit Amster-
dam, 223 pp.

[56] Chappell BW, White AJR. 1992. I-and S-type granites in the Lachlan Fold Belt. Trans.
R. Soc. Edinb. Earth Sci. 83, 1-26.